Biochimica et Biophysica Acta, 1148 (1993) 97–107

BBAMEM 75939

Kinetic study of A-type current inactivation in *Lymnaea* neurons

S.I. Alekseev and A.V. Zaykin

Institute of Cell Biophysics, Russian Academy of Sciences, Puschino, Moscow Region (Russian Federation)

(Received 2 December 1992)

Key words: Voltage clamp; A current; Inactivation kinetics

Macroscopic inactivation of A-current was studied in internally perfused *Lymnaea* neurons under voltage clamp conditions. Inactivation kinetics were satisfactorily described by the sum of two exponentials, suggesting the presence of two type inactivation. The kinetics of recovery from inactivation were exponential. The rate constants of the fast phase of inactivation $\gamma_f(V)$ rose steeply with depolarization exposing the pronounced plateau in the range from −30 to 0 mV. The time course of inactivation in this potential range was more closely approximated with the sum of three exponentially decaying components. Calcium and hydrogen ions strongly affected the fast phase of inactivation. Calcium gave a positive shift of a part of the $\gamma_f(V)$ curve on the left of the plateau. Raising the pH caused a negative shift of the right-hand branch of the $\gamma_f(V)$ curve. It was shown that these effects are associated with Ca^{2+} and H^+ binding to some specific sites of the channel protein. Two models give good fits with the experimental data. They include two pathways for fast inactivation. Calcium and hydrogen ions are assumed to selectively affect the voltage-dependent transitions related to these pathways of inactivation.

Introduction

Transient outward potassium currents or A-currents (I_a) are seen in the membrane of a wide variety of excitable cells [1]. These currents seem to play an important role in the control of the excitability of muscle and neurons [2–5]. In its time course I_a resembles the fast voltage-dependent sodium current more closely [6–9]. Recently, data on the primary structure of A-type channels have become available [10–13]. A site-specific mutagenesis technique applied mainly to *Shaker* potassium channels has made it possible to understand some details of the relations between molecular structure and function in these proteins [14–21].

A comparative study of the kinetics of A-type channels in other preparations could give some insight into the mechanisms underlying gating reactions in these channels. It was shown that the I_a regularly occurs in molluscan neurons. There are published studies of the kinetics of single potassium channels in *Lymnaea* neurons [22,23]. However, little is known about the macroscopic current kinetics.

The aim of the present investigation was to examine the inactivation kinetics of I_a in *Lymnaea* neurons under whole cell voltage-clamp conditions. We have found out that the inactivation kinetics have both general similarities to those of A-currents in other cells and specific differences, which have not been revealed in other types of channels.

Materials and Methods

The experiments were performed on unidentified neurons from the right and left parietal ganglia of *Lymnaea stagnalis*. Experimental procedures employed for intracellular perfusion of isolated neurons, microscopic current recording and curve fitting followed those described by Alekseev [24].

The internal solution contained 80 mM KCl and 10 mM Tris (pH 7.3). The external solution contained (mM): KCl, 1.6 $CaCl_2$, 2; $MgCl_2$, 4; Tris, 45; TEA, 30 (pH 7.5). For one experiment (Fig. 8) pH was adjusted to 9.15. In a study of calcium and magnesium effects the control external solution had the following composition (mM): KCl, 1.6; $CaCl_2$, 4; $MgCl_2$, 16; Tris, 18; TEA, 30. A test solution was made by substituting 4 mM $CaCl_2$ and 16 mM $MgCl_2$ for 16 mM $CaCl_2$ and 4 mM $MgCl_2$ without changing the concentration of the other salts. The pH of both solutions was 7.5. All experiments were performed at 18–20°C.

Correspondence to: S.I. Alekseev, Institute of Cell Biophysics, Russian Academy of Sciences, Puschino, Moscow Region, 142292, Russian Federation.

Abbreviations: TEA, tetraethylammonium chloride; 4-AP, 4-aminopyridine; Tris, tris(hydroxymethyl)aminomethane.

Results

Identification of A-current

A transient outward potassium current in *Lymnaea* neurons distinctly manifests itself only when the conditioning hyperpolarization ($V_c < -80$ mV) precedes the membrane potential V. Otherwise, the transient outward current is entirely inactivated. The optimal conditioning pulse duration was set with the purpose of attaining a new steady-state inactivation level at a given V_c. Fig. 1A–D presents records of this current at various experimental conditions. At potentials tested, the time course of inactivation can be seen to have two distinct phases with different inactivation rates. A considerable part of the slower phase is shown in Fig. 1B at a longer test pulse duration.

The current–voltage relationship for the peak current is shown in Fig. 2A. The transient outward current, from cell to cell, ranges from 0 to 100 nA. In this work we used cells whose current was within 10–50 nA

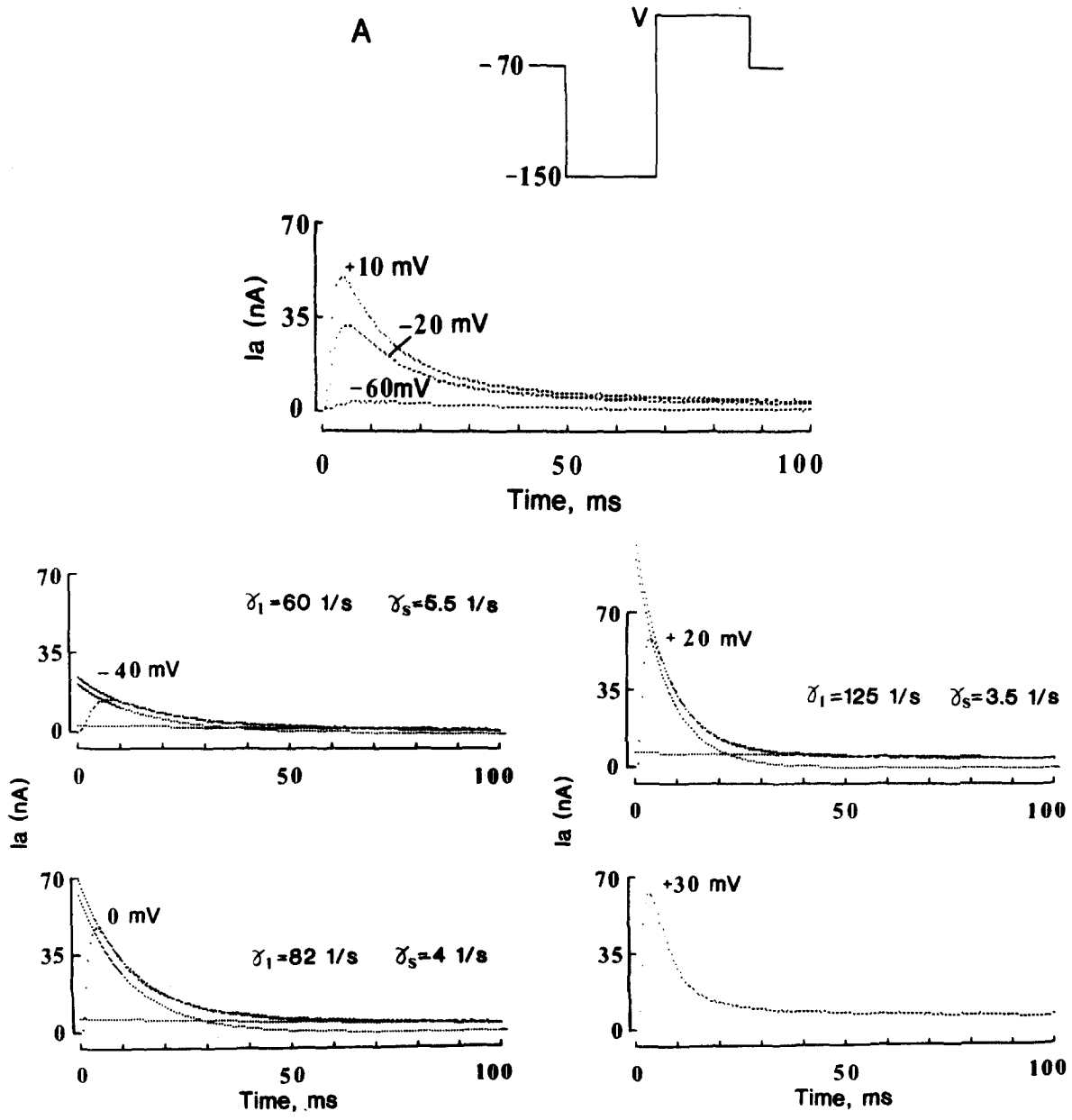

Fig. 1. A-currents under various experimental conditions. (A) Records of currents evoked by depolarizing test pulses of 100 ms duration with preceding hyperpolarizing pulses of 200 ms duration to −150 mV. Pulse protocol, not in scale, is shown in the inset. Traces at −40, 0 and +20 mV are fitted by two exponentials. Individual exponential components are plotted by dashed lines. (B) Example of record of current obtained at test potential of 800 ms duration of 0 mV. (C) Traces of currents at test potentials of −20 mV (1), 0 mV (2) and +20 mV (3), normalized and given in the same scale. (D) Traces of currents obtained at test potential of +20 mV with preceding hyperpolarizing pulses of 200 and 4 ms duration to −150 mV. The trace labeled '4 ms' is shown in lower part in suitable scale. Current traces are fitted by two exponentials.

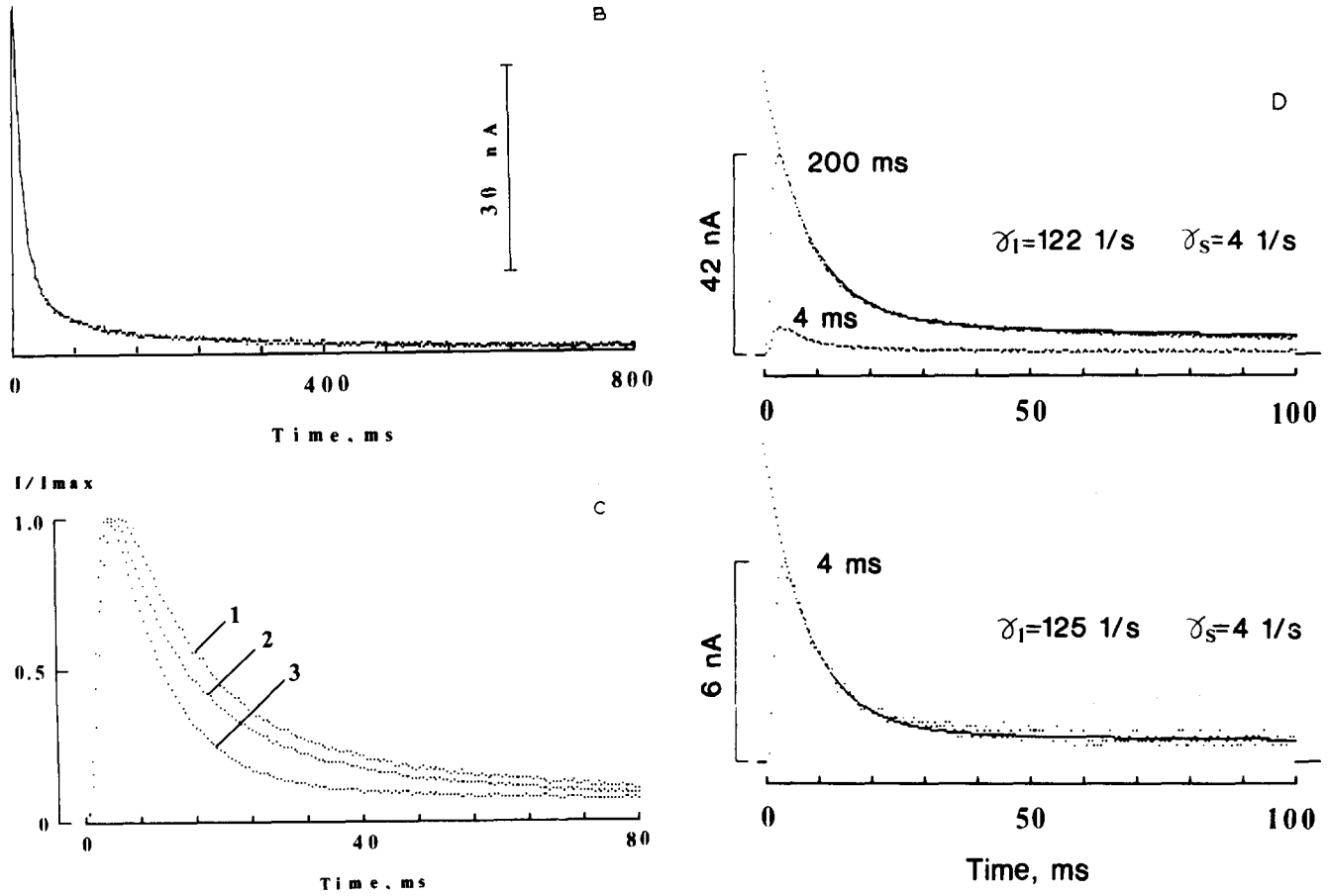

Fig. 1. (continued)

at $V = 0$ mV. Fig. 2B depicts the steady-state inactivation of the transient outward current described by a Boltzmann distribution:

$$h(\infty) = 1/(1+\exp((V-V_0)/d)) \quad (1)$$

where V_0 is membrane potential, at which $h(\infty) = 0.5$, d is a slope factor. Values d and V_c were rather stable for most of the cells investigated: 6.2 ± 0.2 mV and -95 ± 5 mV, respectively. In each particular cell V_0 and d not depend either on the test potential within -50–30 mV or on the way they were obtained (by peak current or by current values at 120 ms).

When in the internal solution, K^+ ions were replaced by Cs^+, the transient outward current was entirely suppressed. Addition of 10 mM 4-AP to the external solution led to blocking of the transient outward current in many cells by approx. 90%. At the same time the blocking effect of TEA (to 30 mM) was not expressed. The transient outward current observed in *Lymnaea* neurons is, according to its properties, similar to A-currents (I_a) in other cells [6–9]. So, like other authors we denoted the observed potassium current by I_a.

Approaches to description of kinetics

Over a wide range of the potentials studied, the kinetics were best described by a two-exponential expression:

$$h(t) = C_0 + C_f \cdot \exp(-\gamma_f \cdot t) + C_s \cdot \exp(-\gamma_s \cdot t) \quad (2)$$

where C_0 is constant, C_f and C_s are the relative contributions of both exponential functions, and γ_f and γ_s are the rate constant of the rapidly decaying and the slowly decaying current components, respectively.

At short test pulse durations (100–400 ms) the slow phase of inactivation kinetics is obscured by the fast one. For a detailed study of the slow phase we used more prolonged traces of I_a lasting for 800–1400 ms. A part of decaying current, beginning 150 ms after the test pulse onset, was described by a single exponential. It was then subtracted from the current trace recorded at a test pulse duration of 100–200 ms. The difference curve was adequately approximated by a single exponential (SD near 0.0061 s^{-1} at $V = -10$ mV), but in the potential range from -30 to 10 mV it was more closely approximated by a two-exponential function (Eqn. 2) (SD near 0.0035 s^{-1} at $V = -10$ mV). In the

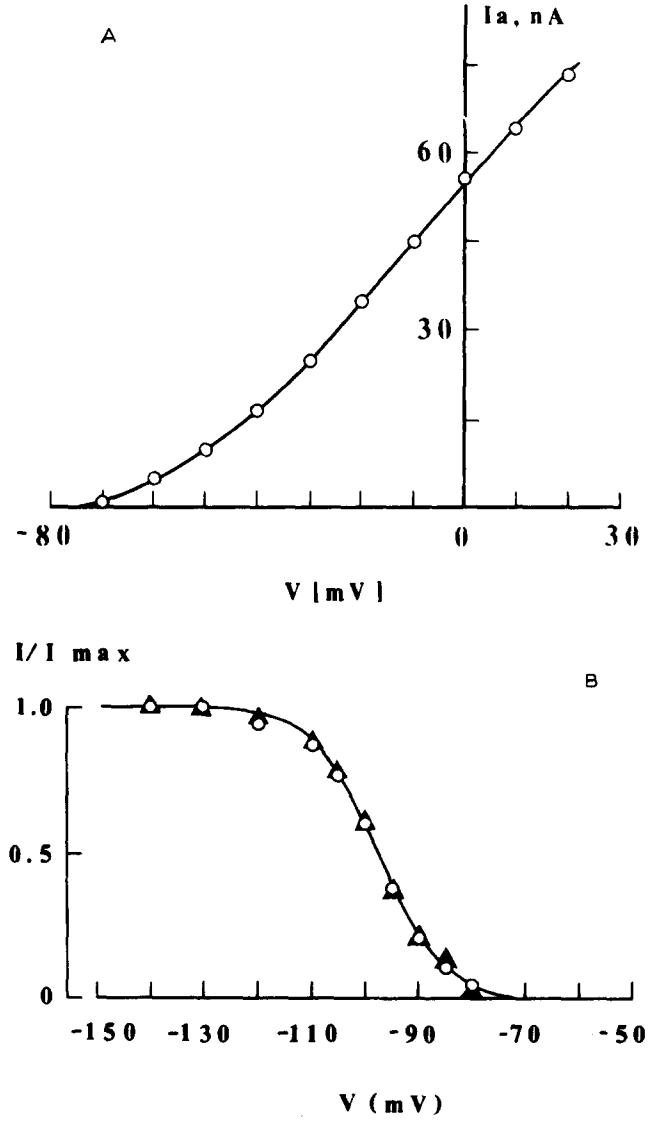

Fig. 2. (A) Peak current-voltage relationship and (B) voltage dependence of steady-state inactivation of I_a obtained from measurements of peak currents during test pulses (circles) and current magnitude at 120 ms after the test pulse onset (triangles). This interval was chosen to record only a slow decaying phase of the current. The solid line is a fit with Eqn. 1 at $V_0 = -97$ mV and $d = 6.2$ mV.

latter case the function describing the kinetics could be written as follows:

$$h(t) = C_0 + C_1 \cdot \exp(-\gamma_1 \cdot t) + C_2 \cdot \exp(-\gamma_2 \cdot t) + C_s \cdot \exp(-\gamma_s \cdot t) \quad (3)$$

The kinetics of recovery from inactivation are approximated with a single exponential: $h(t) = 1 - \exp(-\gamma_r t)$. Examples of the fit are shown in Fig. 3A.

The effects of fitting the two-exponential function (Eqn. 2) to decay portions of the currents and to time courses of the development of inactivation obtained in the double-pulse experiment are illustrated in Figs. 1A, D and Fig. 3B, respectively. The kinetics obtained by

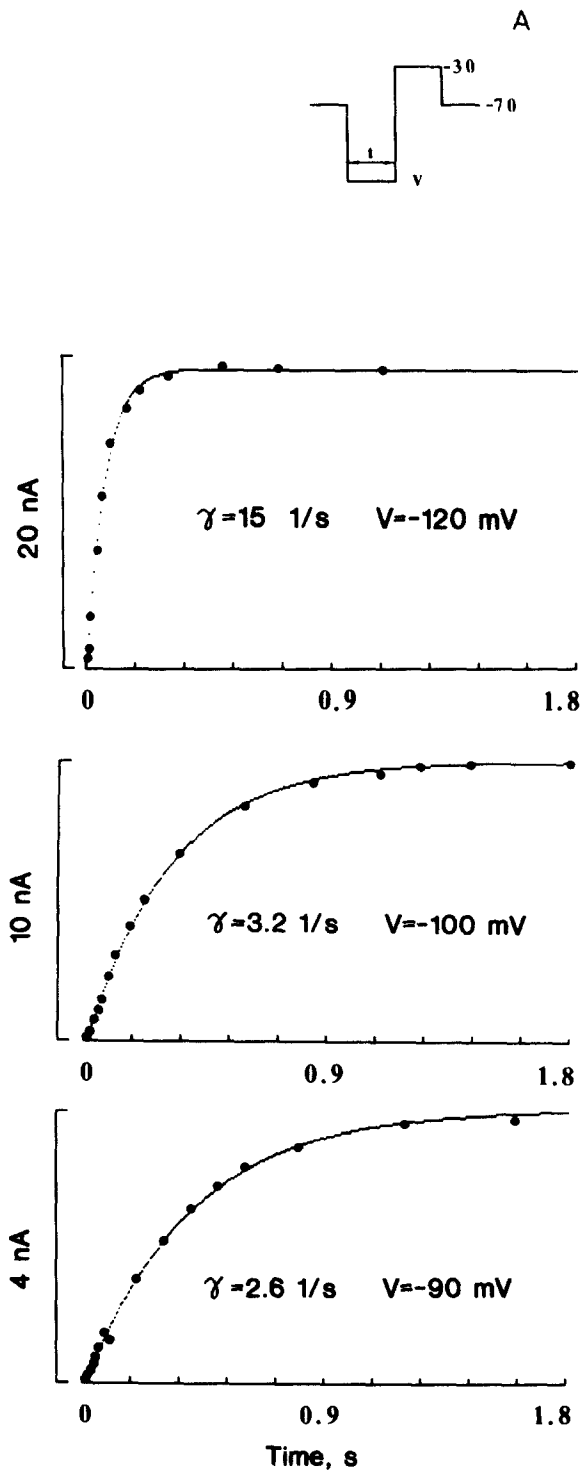

Fig. 3. Time course of removal (A) and development (B) of inactivation. Curves drown through the data points are least-squares fits. Kinetics of development of inactivation are fitted by two exponentials. The rate constants and related pulse protocols are indicated.

both methods yielded similar rate constants at the given potentials.

Potential dependence

Potential dependence of the rate constants of development and removal of inactivation is illustrated in

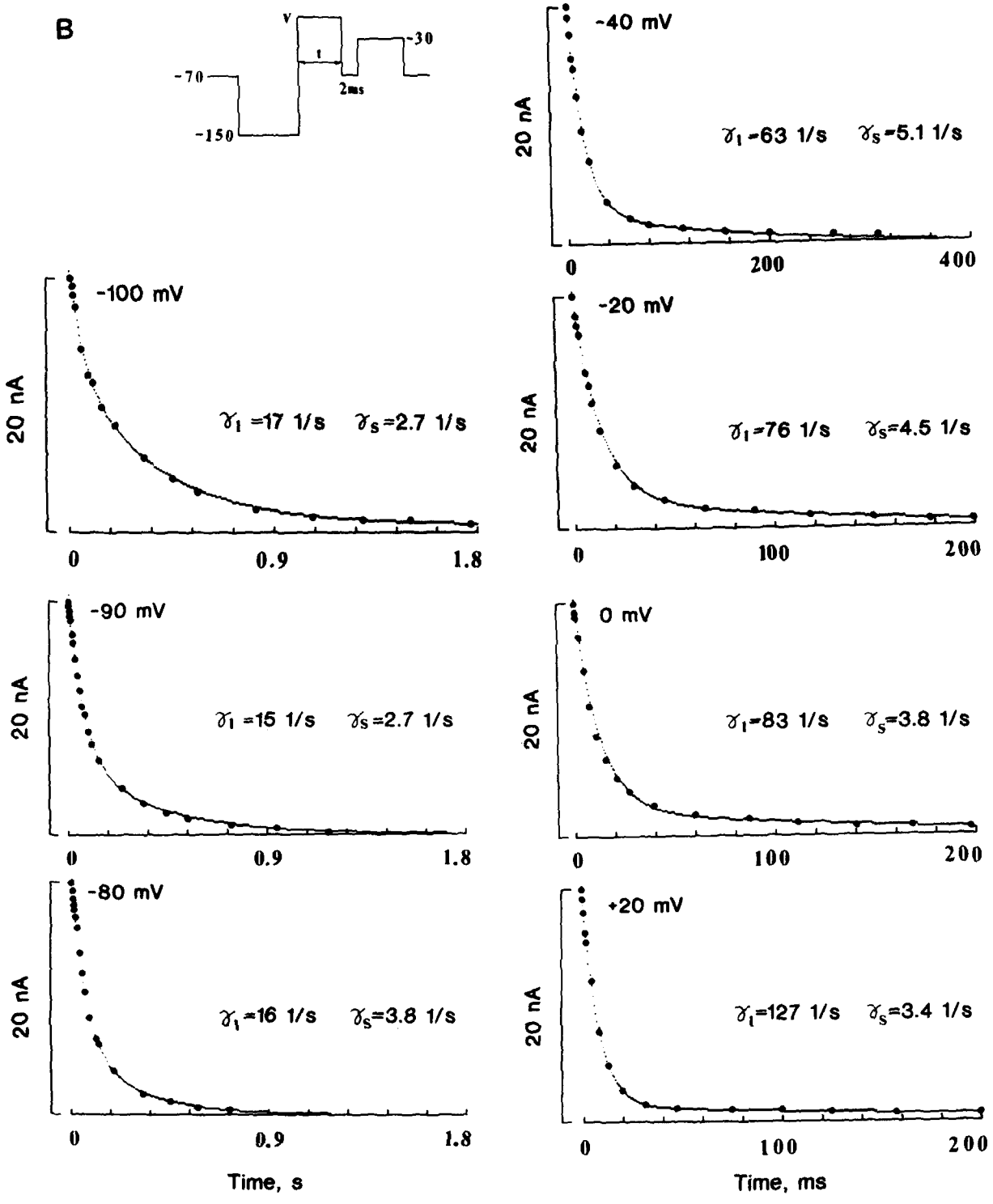

Fig. 3. (continued)

Figs. 4A–C. Note that there are some peculiarities in these curves. In the range from −60 to 30 mV the $\gamma_s(V)$ curve shows little dependence on the potential (Figs. 4A, B). In the case of the two-exponential fit the $\gamma_f(V)$ curve increased steeply at potentials between −90 and −30 mV and more positive than at about 0 mV (Fig. 4B). In the range between −30 and 0 mV the $\gamma_f(V)$ curve had a pronounced plateau. The $\gamma_r(V)$ curve was coupled to the $\gamma_s(V)$ curve rather than to the $\gamma_f(V)$ one and tended to saturation at potentials more negative than −180 mV. At the same V the γ_f values always lay above the γ_r ones. This difference is authentic and was observed in all the cells investigated. The appropriate kinetics are shown in Figs. 3A, B.

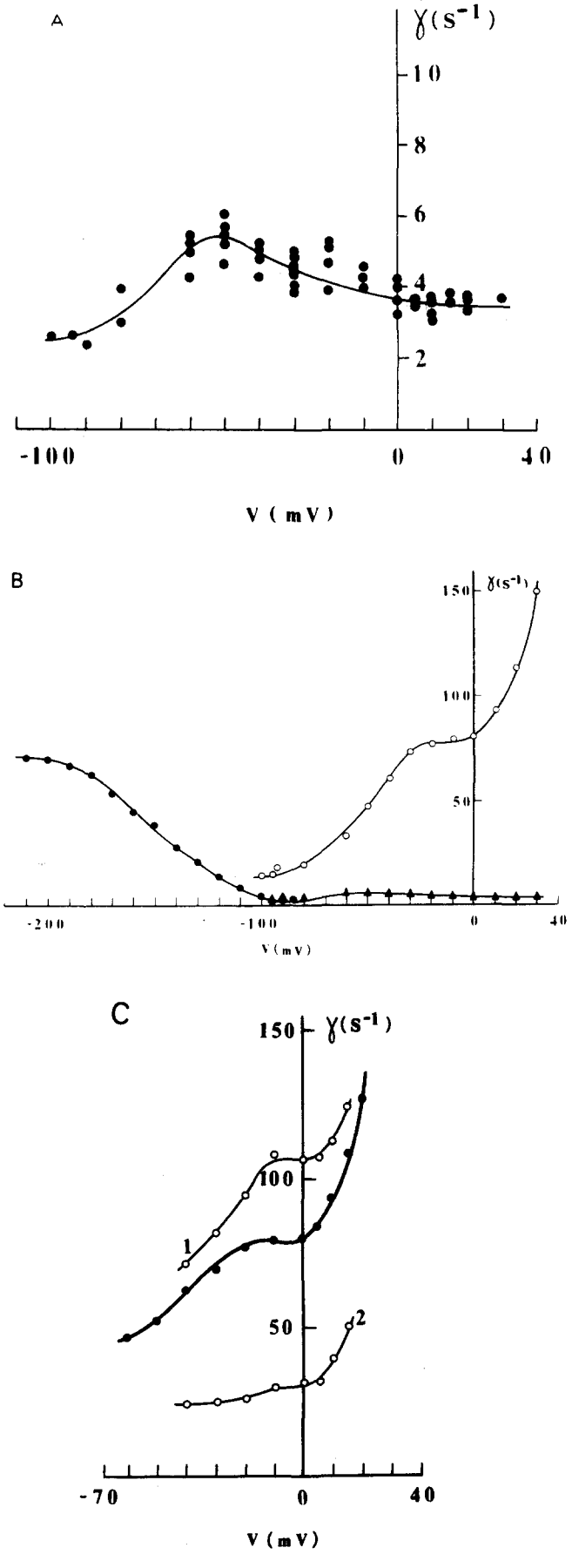

Fig. 4C demonstrates rate constants obtained from the three-exponential fit to the inactivation kinetics. As can be seen, the $\gamma_1(V)$ curve behaves without any considerable qualitative changes. The typical plateau revealed in the case of the two-exponential approximation remains. The potential dependence of γ_2 is qualitatively similar to that of γ_1.

As can be seen in Fig. 1C, the decaying phases of current traces at -20 mV and at 0 mV differ slightly while the decay of current at $+20$ mV is markedly different from the first two. Also, the peaks of currents are monotonically shifted towards the onset of the test pulse when the potential increases. This indicates that the activation rate of I_a, in contrast to the inactivation rate, increases monotonically as V becomes more positive. The potential dependence of the activation time constants did not reveal a plateau in the range from -30 to 0 mV as well [25]. Thus, it is reasonable to suggest that the observed rate limitation is intrinsic only to inactivation of I_a.

The variations of pre-exponential coefficients with the potential are represented in Figs. 5A, B. At any given test potentials the ratio between C_f and C_s remains unchanged when the conditioning prepulse is varied from -100 to -180 mV. C_0 was near zero throughout the potential range studied.

The standard deviation of the decay portion of I_a obtained from fitting curves is dependent on the potential (Fig. 6). It is seen that the S.D. increases with the negative membrane potential which is due to a decrease in current amplitude and, hence, in signal-to-noise ratio. At potentials more negative than -30 mV and more positive than 10 mV the kinetics are described equally well by either Eqn. 2 or Eqn 3. Yet, within the -30 mV to $+10$ mV range of the plateau the error in description of the kinetics by Eqn 3 is less when Eqn. 2 is used; i.e., a noticeable deviation of the kinetics from the two exponentials is observed. An equal description of kinetics by both functions beyond this range appears to be related to a decrease of contribution of the second component C_2, which brings Eqn. 3 closer to a two-exponential form. Further on, to simplify an analysis we will use the two-exponential approximation of the inactivation kinetics.

Fig. 1D showed traces of I_a obtained under conditions of possible contamination with the delayed rectifier current ($V = +20$ mV). Shortening of the hyperpo-

Fig. 4. Rate constants of inactivation of I_a as a function of voltage. (A) Rate constants of slow phase of inactivation obtained from six cells. (B) Rate constants γ_f (open circles) and γ_s (triangles) obtained from a two-exponential fit to the inactivation kinetics. Full circles are rate constants of removal of inactivation. (C) Rate constants γ_1 (curve 1) and γ_2 (curve 2) of a three-exponential fit to the inactivation kinetics. Rate constants γ_f obtained from a two-exponential fit to the same kinetics are given as full circles.

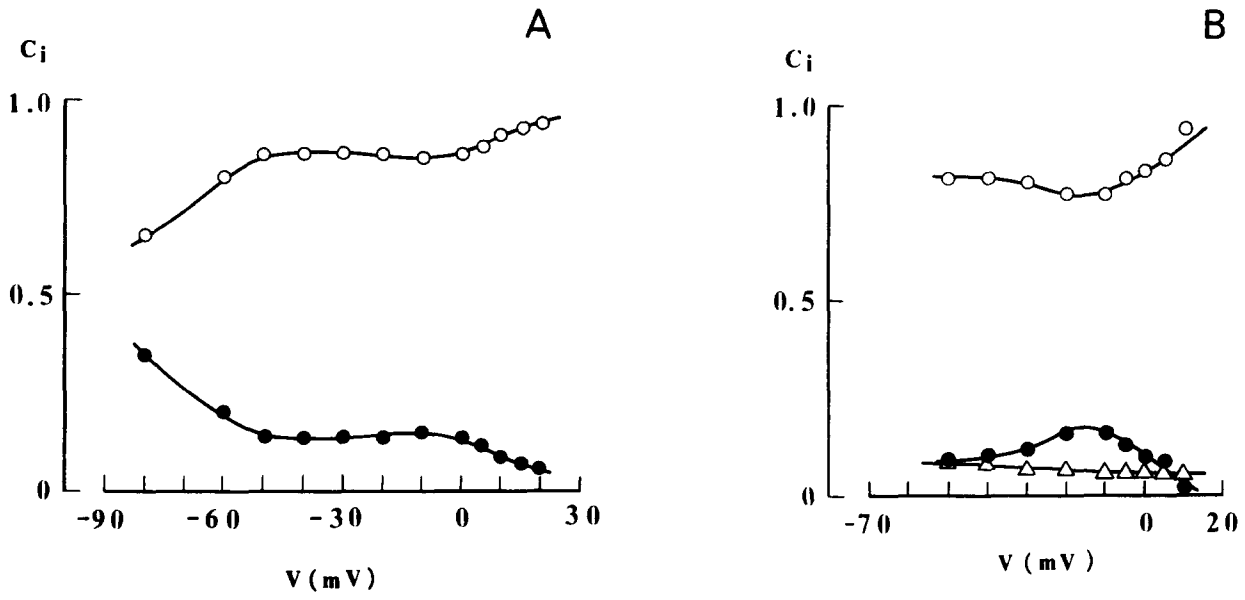

Fig. 5. Potential dependence of normalized pre-exponential coefficients. (A) C_f (open circles) and C_s (full circles) are obtained from a two-exponential fit to the inactivation kinetics. (B) C_1 (open circles), C_2 (full circles) and C_s (triangles) are obtained from a three-exponential fit to the same inactivation kinetics.

larizing prepulse duration from 200 ms to 4 ms resulted in a decrease of the current amplitude about 7 times without significant change in the rate constants. The S.D. value of mean γ_f from five cells tested was $\pm 6\%$. We suppose that the ionic currents other than I_a could not be affected by the prepulse duration. Hence, at the shorter prepulse duration their relative magnitudes would have risen. The small changes in the rate constants indicate that the contamination of I_a by other ionic currents under given experimental conditions seems to be minimal. The good agreement between the rate constants of the inactivation kinetics obtained in the double-pulse experiment and from current decay also supports this view. Also, the presence of the plateau did not appear to be an artifact by a series resistance of the pipette, since its width did not correspond with the size of the cell under study, and, hence, with a I_a change in the range of 10–100 nA.

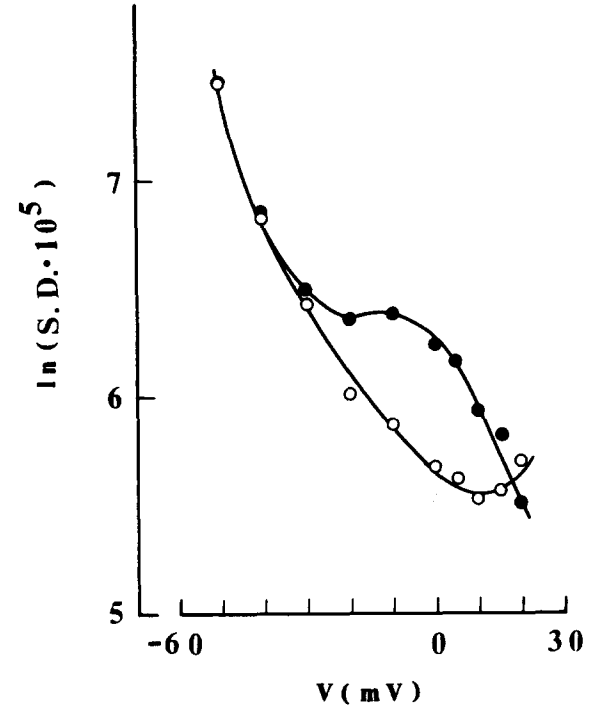

Fig. 6. Potential dependence of the standard deviation of the decaying portions of normalized currents obtained from fitting by the sum of two (full circles) and three (open circles) exponentials.

Effects of divalent cations

Replacement of 4 mM Ca^{2+} and 16 mM Mg^{2+} with 16 mM Ca^{2+} and 4 mM Mg^{2+} in the external solution (see Methods) resulted in an appreciable fall of the current amplitude and the inactivation rate depending on the test potential (Fig. 7A). At the same time the kinetics of recovery from inactivation were not sensitive to this replacement (Fig. 7B). As can be seen in Fig. 7C, the only effect of the replacement of divalent cations on the fast phase of inactivation is a shift of the rising branch of the $\gamma_f(V)$ curve on the left of the plateau in a depolarizing direction by about $11(\pm 3)$ mV. This resulted in an apparent reduction of the plateau width. Calcium and magnesium replacement had little effect on the rate constants of the slow phase of inactivation. The steady-state inactivation and activation curves were shifted in a depolarizing direction by 10 ± 2 mV and 11 ± 3 mV, respectively.

Thus, the rates of development and removal of inactivation can be changed independently. Moreover,

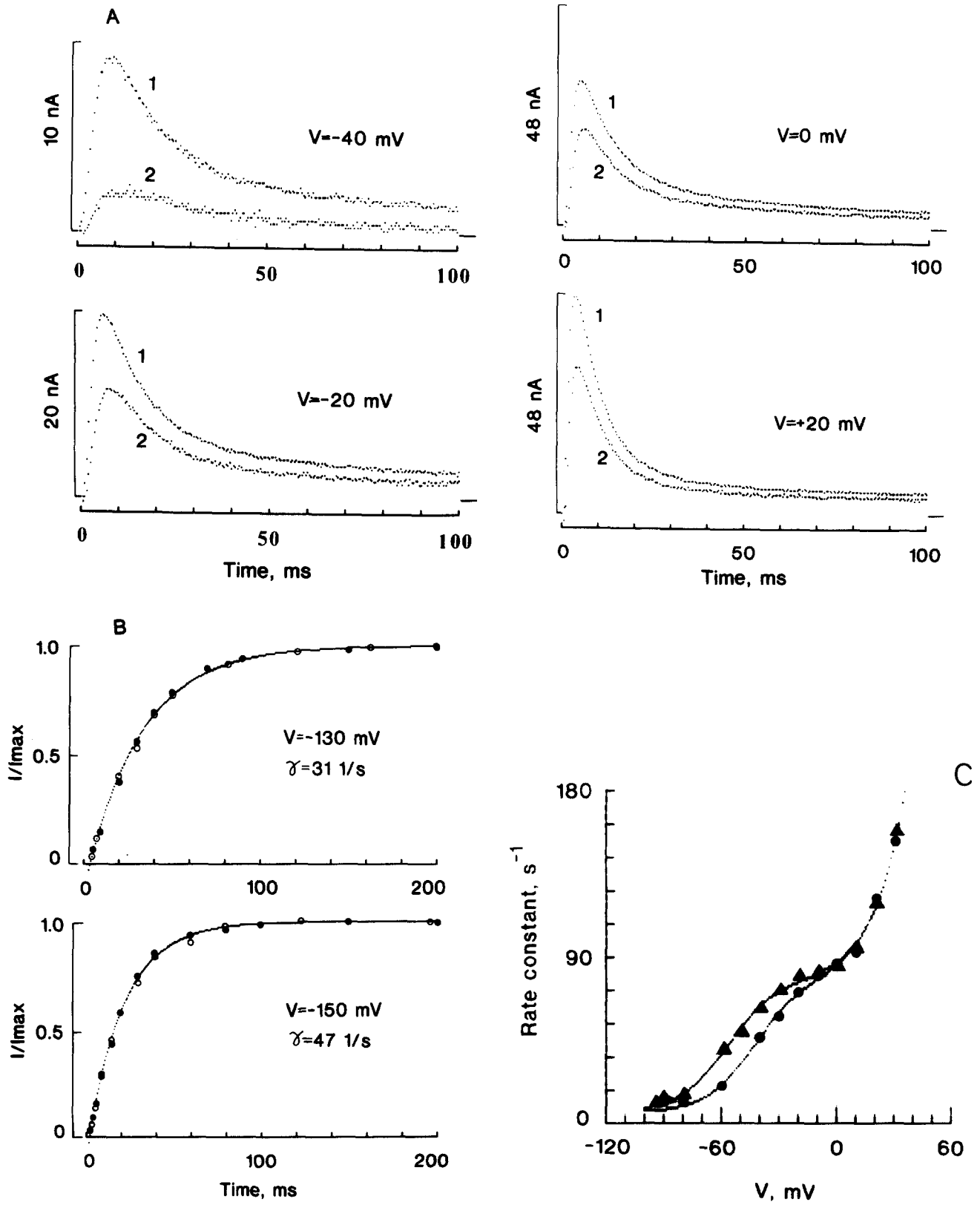

Fig. 7. Effects of divalent cations on inactivation. (A) Superimposed traces show currents recorded in two external solutions containing either 4 mM Ca^{2+} and 16 mM Mg^{2+} (traces 1) or 16 mM Ca^{2+} and 4 mM Mg^{2+} (traces 2) at various depolarizing test potentials indicated. (B) Time courses of removal of inactivation obtained in the same external solutions as in A with preceding hyperpolarizing pulses to −130 and −150 mV. Open circles are measurements in the solution with higher Ca^{2+} concentration. Continuous curves are superimposed least-squares fits. (C) Voltage dependence of the rate constants of the fast phase of inactivation in neurons bathed with the same external solutions as in A. Full circles are measurements in the solution with a higher Ca^{2+} concentration. The smooth curves are fits with model I.

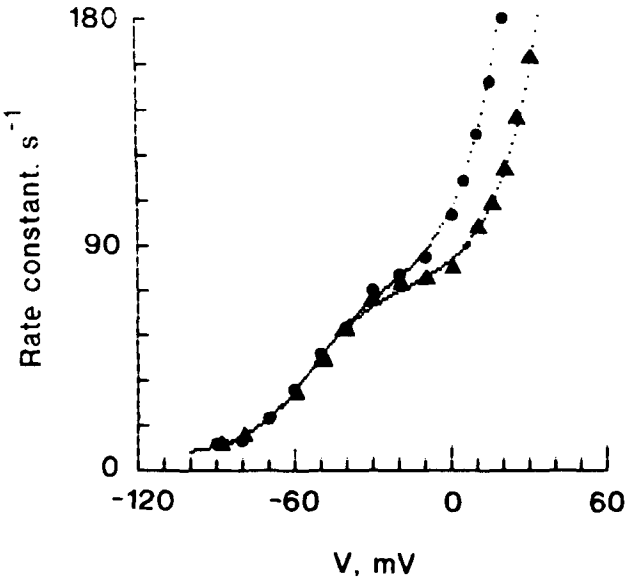

Fig. 8. The rate constants of the fast phase of inactivation at pH 7.5 (triangles) and 9.15 (circles). The smooth curves were determined from model I.

the $\gamma_f(V)$ curve is also not monotonous. Its two rising branches can be shifted in a different fashion.

Sensitivity to pH changes

The effect of pH on the inactivation rate was strongly dependent on the membrane potential. Raising the pH from 7.5 to 9.15 has almost no effect on the left-hand branch of the $\gamma_f(V)$ curve (Fig. 8) as well as the rate constants of the slow phase of inactivation and recovery from inactivation. Steady-state activation and inactivation were also not affected by the pH changes. On the other hand, the right-hand branch of the $\gamma_f(V)$ curve was displaced 16 ± 3 mV to the left for pH 9.15 (Fig. 8). This result confirms our previous finding that the two branches of the $\gamma_f(V)$ curve on the left and on the right of the plateau can be shifted independently.

Discussion

The inactivation kinetics of A-current in *Lymnaea* neurons, on the whole, were described satisfactorily by the two-exponential function. Complex inactivation kinetics were found to be typical for A-currents in many preparations including *Shaker* potassium channels [26–31].

The application of site-specific mutagenesis to *Shaker* potassium channels has made it possible to understand molecular mechanisms of inactivation in this preparation [18–21]. It was found that two different types of inactivation, N- and C-type, are responsible for fast and slow phases of the inactivation kinetics. N-Type inactivation is fast and occurs by a process whereby the intracellular region of the amino terminus occludes the internal mouth of the channel. C-Type inactivation can be seen as a slow decay in the macroscopic current remaining after the fast phase of inactivation. The rate of C-type inactivation is independent of voltage. The molecular mechanism of C-type inactivation is distinct from that of N-type inactivation and is assumed to involve the constriction of the external mouth of the channel [21].

Inactivation of A-current in *Lymnaea* with multiple exponential components also suggests the presence of multiple inactivation processes in this preparation. As the properties of the slow phase of inactivation are very similar to that of *Shaker* potassium channels, a process similar to C-type inactivation may be responsible for the slow phase of A-current inactivation in *Lymnaea* as well. However, the potential dependence of the fast phase of inactivation is different from that of *Shaker* potassium channels. Therefore, similarity in the mechanisms of the fast phases of inactivation in these two preparations is not so evident.

To interpret the potential dependence of the fast phase of inactivation, we have used a partial kinetic scheme according to Aldrich and co-workers [21,23]. Two types of kinetic scheme give a good agreement with the experimental results. In Schemes I and II C represents the many closed states from which the channel undergoes transitions to open states, O, O_1 and O_2; I_1 and I_2 are inactivated states of channel. k_i and λ_i are potential-independent inactivation rate constants. The voltage dependence of the other rate constants are constrained by the following equations (e.g., Ref. 33):

$$\alpha_{\pm i} = \alpha_{0i} \cdot \exp[\pm A_i(V - V_{0i})] \text{ and } \delta_{\pm 1} = \sigma_{01} \cdot \exp[\pm D_1(V - V_{0d})] \quad (4)$$

This form of rate constant presentation is very useful in modeling the effects of Ca^{2+} and H^+ on the potential-dependent parameters of the channel. Each model was described by a set of ordinary differential equations similar to those used, for example, in Ref. 34. Numerical solutions of these equations predict the

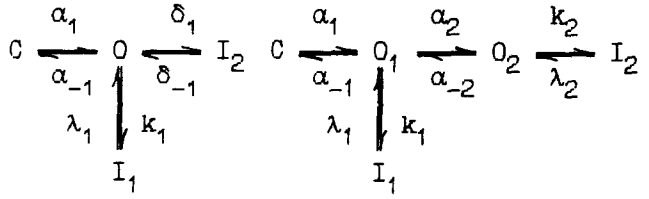

Scheme I Scheme II

appearance of the plateau in the $\gamma_f(V)$ curve at the following magnitude of the rate constants (s^{-1}):

$$\alpha_{\pm 1} = 200 \cdot \exp[\pm 0.04(V+58)], \quad \alpha_{\pm 2} = 200 \cdot \exp[\pm 0.03(V-30)]$$

$$\delta_{\pm 1} = \exp[\pm 0.06(V+43)], k_1 = 70, \lambda_1 = 6, k_2 = 300, \lambda_2 = 0.01.$$

The effect of substituting 4 mM Ca^{2+} and 16 mM Mg^{2+} for 16 mM Ca^{2+} and 4 mM Mg^{2+} was reproduced in both models by changing V_{01} from -58 mV to -46 mV. This resulted in a positive shift of the steady-state activation curve by 12 mV which is in close agreement with the experimental data. Fits with model I are shown in Fig. 7C. Model II also gives good fits with $\gamma_f(V)$ curves. The shift in the right-hand branch of the $\gamma_f(V)$ curve caused by raising pH was reproduced in model I by changing V_{0d} from -45 to -60 mV (Fig. 8) and in model II by changing V_{02} from 30 to 15 mV, respectively. The slow phase of inactivation can be described in both models by adding separate pathways of inactivation from an open state in accordance with the scheme for N- and C-type inactivation proposed by Hoshi et al. [21].

Thus, these models satisfactorily describe the effects of divalent cations and pH on the fast phase of inactivation. According to both Schemes, the channel can close to an inactivated state (I_1) at the same transition rate, k_1. This type of inactivation is potential independent and seems to be similar to the N-type inactivation described by Hoshi et al. [21]. Scheme I predicts that at $V > 0$ the channel can undergo rapid potential-dependent inactivation by an exclusive mechanism. An obvious alternative to the proposed N-type inactivation is the idea that the separate gate controlled by the gating charge is responsible for this type of inactivation. In Scheme II closing the channel to inactivated state I_2 is preceded by the rapid transition of the channel between two open states, O_1 and O_2. Inactivation from the O_2 state is potential independent and can be caused either by the same mechanism as inactivation from the O_1 state (probably N-type) or by a different one. The magnitude of the transition rate constant k_2 is very critical for a slope of the rising branch of the $\gamma_f(V)$ curve on the right of the plateau and is found to be much larger than k_1. This finding does not contradict, however, the assumption that a single type of inactivation underlies both transitions, k_1 and k_2, as the difference between k_1 and k_2 may be caused by conformational changes of channel protein during $O_1 \rightarrow O_2$ transition. At present, we can not definitely distinguish between Schemes I and II. Moreover, some parameters of these partial schemes (e.g., λ_i, α_{02}) should be admitted as being preliminary. Elaboration of an expanded scheme and single-channel recordings should be of help in accurate calculation of these parameters.

Both models include two pathways for fast inactivation. Scheme I predicts that the third type of inactivation may be responsible for A-current decay at $V > 0$ mV. It appears that this type of inactivation is controlled by voltage-dependent gating apparatus which is sensitive to the external H^+ concentration. For Scheme II the presence of the third type of inactivation remains to be shown. The high selectivity of the effect of hydrogen ions on the only voltage-dependent characteristic of the channel, $\gamma_f(V)$, means that:

(a) changes in pH from 7.5 to 9.15 do not affect a surface potential as the uniform fixed charge theory predicts equivalent shifts of all the voltage-dependent characteristics of the ionic channels [35–37];

(b) hydrogen ions seem to interact with basic groups electrically close to gating apparatus ($O \rightarrow I_2$ or $O_1 \rightarrow O_2$) [38,39];

(c) this gating apparatus is located far enough from the activation voltage sensor to influence it. The role of the voltage-dependent transition, $O_1 \rightarrow O_2$ is not clear. This transition seems to involve movement of charged particles through the membrane field but not to be associated with the S4 mechanism of voltage-dependent activation gating [40]. Otherwise, the pH changes could affect activation gating too.

The effect of divalent cations on the kinetics can be explained either by non-specific screening of a fixed negative charge on the surface membrane or by specific binding to a negatively charged group of the channel protein, or to electrically close phospholipids [30,39,41–43]. Since the total concentrations of mono- and divalent cations were equal in both solutions the effect of the replacement of divalent cations on the voltage-dependent characteristics of the channel due to non-specific screening of fixed negative charge should be minimal. Hence, the shifts of $h(\infty)$ and the left-hand branch of the $\gamma_f(V)$ curve which were correlated with the enhancement of calcium rather than magnesium could be caused by specific binding of calcium to negatively charged groups related to the channel protein. An effect interpreted in this way has been reported for sodium and potassium channels [30,42,43]. The models predict that the positive shift of the left-hand branch of the $\gamma_f(V)$ curve can result from the calcium effect on the activation transition rate constants. This means that an interaction of calcium with a negatively charged element of the activation gating apparatus may be mainly responsible for the calcium effect on the inactivation kinetics.

Acknowledgement

We thank Dr. A.S. Kharitonov for technical assistance in preparation of this manuscript.

References

1 Rogawski, M.A. (1985) Trends Neurosci. 8, 214–219.
2 Connor, J.A. and Stevens, C.F. (1971) J. Physiol. 213, 31–53.
3 Daut, J. (1973) Nature New Biol. 246, 193–196.
4 Connor, J.A. (1975) J. Neurophysiol. 38, 922–932.
5 Connor, J.A. (1978) Fed. Proc. 37, 2139–2145.
6 Neher, E. (1971) J. Gen. Physiol. 58, 36–53.
7 Connor, J.A. and Stevens, C.F. (1971) J. Physiol. 213, 21–30.
8 Thompson, S.H. (1977) J. Physiol. 265, 465–488.
9 Belluzzi, O., Sacchi, O. and Wanke, E. (1985) J. Physiol. 358, 91–108.
10 Baumann, A., Krah-Jentgens, I., Müller, R., Müller-Holtkamp, F., Seidel, R., Kecskemethy, N., Casal, I., Ferrus, A. and Pongs, O. (1987) EMBO J. 6, 3419–3429.
11 Tempel, B.L., Papazian, D.M., Schwarz, T.L., Jan, Y.N. and Jan, L.Y. (1987) Science 237, 770–775.
12 Schwarz, T.L., Tempel, B.L., Papazian, D.M., Jan, Y.N. and Jan, L.Y. (1988) Nature 331, 137–142.
13 Pongs, O., Kecskemethy, N., Müller, R., Krah-Jentgens, I., Baumann, A., Kiltz, H.H., Casal, I., Uamazares, S. and Ferrus, A. (1988) EMBO J. 7, 1087–1096.
14 Iverson, L.E., Tanouye, M.A., Lester, H.A., Davidson, N. and Rudy, B. (1988) Proc. Natl. Acad. Sci. USA 85, 5723–5727.
15 Timpe, L.C., Schwarz, T.L., Tempel, B.L., Papazian, D.M., Jan, Y.N. and Jan, L.Y. (1988) Nature 331, 143–145.
16 Timpe, L.C., Jan, Y.N. and Jan, L.Y. (1988) Neuron 1, 659–667.
17 McCormack, K., Tanouye, M.A., Iverson, L.E., Lin, J.W., Ramaswami, M., McCormack, T., Campanelli, J.T., Mathew, M.K. and Rudy, B. (1991) Proc. Natl. Acad. Sci. USA 88, 2931–2935.
18 Hoshi, T., Zagotta, W.N. and Aldrich, R.W. (1990) Science 250, 533–538.
19 Zagotta, W.N., Hoshi, T. and Aldrich, R.W. (1990) Science 250, 568–571.
20 Choi, K.L., Aldrich, R.W. and Yellen, G. (1991) Proc. Natl. Acad. Sci. USA 88, 5092–5095.
21 Hoshi, T., Zagotta, W.N. and Aldrich, R.W. (1990) Neuron 7, 547–556.
22 Kazachenko, V.N. and Geletyuk, V.I. (1984) Biochim. Biophys. Acta 773, 132–142.
23 Geletyuk, V.I. and Kazachenko, V.N. (1987) Biophysics (Moscow) 32, 859–873.
24 Alekseev, S.I. (1992) Biochim. Biophys. Acta 1110, 178–184.
25 Alekseev, S.I. (1993) Biol. Membr. (Moscow) 10, N4, in press.
26 Cooper, E. and Shrier, A. (1989) J. Gen. Physiol. 94, 881–910.
27 Solc, C.K. and Aldrich, R.W. (1990) J. Gen. Physiol. 96, 135–165.
28 Kasai, H., Kameyama, M., Yamaguchi, K. and Fukida, J. (1986) Biophys. J. 49, 1243–1247.
29 Solc, C.K., Zagotta, W.N., Aldrich, R.W. (1987) Science 236, 1094–1098.
30 Mayer, M.L. and Sugiyama, K. (1988) J. Physiol. 396, 417–433.
31 Apkon, M. and Nerbonne, J.M. (1991) J. Gen. Physiol. 97, 973–1011.
32 Zagotta, W.N. and Aldrich, R.W. (1990) J. Gen. Physiol. 95, 29–60.
33 Keynes, R.D. and Rojas, E. (1976) J. Physiol. 255, 157–189.
34 Aldrich, R.W. (1981) Biophys. J. 36, 519–532.
35 Frankenhaeuser, B. and Hodgkin, A.L. (1957) J. Physiol. 137, 218–244.
36 McLaughlin, S.G.A., Szabo, G. and Eisenman, G. (1971) J. Gen. Physiol. 58, 667–687.
37 Hahin, R. and Campbell, D.T. (1983) J. Gen. Physiol. 82, 785–802.
38 Hille, B. (1968) J. Gen. Physiol. 52, 221–236.
39 Hille, B., Woodhull, A.M. and Shapiro, B.I. (1975) Philos. Trans. R. Soc. B 270, 301–318.
40 Stühmer, W., Conti, F., Suzuki, H., Wang, X., Noda, M., Yahagi, N., Kubo, H., Numa, Sh. (1989) Nature 339, 597–603.
41 Shoukimas, J.J. (1978) J. Membr. Biol. 38, 271–289.
42 Gilly, W.F. and Armstrong, C.M. (1982) J. Gen. Physiol. 79, 935–964.
43 Gilly, W.F. and Armstrong, C.M.; (1982) J. Gen. Physiol. 79, 965–996.